JBC Papers in Press. Published on June 10, 2002 as Manuscript M203275200

Synthetic Miniprion PrP106

Valentina Bonetto[1]*, Tania Massignan[1], Roberto Chiesa[1], Michela Morbin[2], Giulia Mazzoleni[2], Luisa Diomede[1], Nadia Angeretti[1], Laura Colombo[1], Gianluigi Forloni[1], Fabrizio Tagliavini[2], and Mario Salmona[1]

[1] Istituto di Ricerche Farmacologiche "Mario Negri", via Eritrea 62, 20157 Milan, Italy.

[2] Istituto Neurologico "Carlo Besta", via Celoria 11, 20133 Milan, Italy.

*****To whom correspondence should be addressed. Tel. No. +39-0239014548; Fax No. +39-023546277; e-mail address: bonetto@marionegri.it

Running title: Synthetic miniprion PrP106

SUMMARY

Elucidation of structure and biological properties of PrP^{Sc} is fundamental to understand the mechanism of conformational transition of PrP^{C} into disease-specific isoforms and the pathogenesis of prion diseases. Unfortunately, the insolubility and heterogeneity of PrP^{Sc} have limited these studies. The observation that a construct of 106 amino acids (termed PrP106 or miniprion) derived from mouse PrP and containing two deletions (Δ23-88, Δ141-176), becomes protease-resistant when expressed in scrapie-infected neuroblastoma cells and sustains prion replication when expressed in $PrP^{0/0}$ mice, prompted us to generate a corresponding synthetic peptide (sPrP106) to be used for biochemical and cell culture studies. sPrP106 was successfully obtained with a straightforward procedure, which combines classical stepwise solid-phase synthesis with a purification strategy based on transient labelling with a lipophilic chromatographic probe. sPrP106 readily adopted a β-sheet structure, aggregated into branched filamentous structures without ultrastructural and tinctorial properties of amyloid, exhibited a proteinase K-resistant domain spanning residues 134-217, was highly toxic to primary neuronal cultures and induced a remarkable increase in membrane microviscosity. These features are central properties of PrP^{Sc} and make sPrP106 an excellent tool to investigate the molecular basis of the conformational conversion of PrP^{C} into PrP^{Sc} and prion disease pathogenesis.

INTRODUCTION

Prion-related encephalopaties are characterized by accumulation of pathogenic forms of the prion protein (PrP)[1], termed PrP scrapie (PrP^{Sc}), in the central nervous system. Unlike the normal cellular isoform (PrP^{C}), PrP^{Sc} has a high content of β-sheet secondary structure, is insoluble in non-denaturing detergents and partially resistant to protease digestion, and has the propensity to form amyloid fibrils. Elucidation of the structure of both PrP isoforms is fundamental to understand the molecular mechanism of the conformational transition from PrP^{C} to PrP^{Sc}. Unfortunately structural studies of the pathogenic form have been hampered by the insolubility, heterogeneity and complexity of PrP^{Sc} preparations. Synthetic and recombinant fragments of PrP have been more useful for such investigations (1). A construct of 106 amino acids (designated as PrP106 or miniprion), derived from mouse PrP and containing two deletions (Δ 23-88, Δ 141-176), was expressed in scrapie-infected neuroblastoma cells generating a protease resistant polypeptide, displaying better solubility

[1] The abbreviations used are: PrP, prion protein; PrP^{C}, cellular isoform of PrP; PrP^{Sc}, scrapie isoform of PrP; rPrP106, recombinant PrP106; sPrP106, synthetic PrP106; dsPrP106, derivatized synthetic PrP106; PK, proteinase-K ; SSPS, stepwise solid-phase synthesis; Fmoc, N-(9-fluorenyl)methoxycarbonyl; TFE, trifluoroethanol; DCM, dichloromethan; TFA, trifluoroacetic acid; RP-HPLC, reverse-phase HPLC; MALDI MS, matrix-assisted laser desorption/ionization mass spectrometry; TEA, triethylamine; CD, circular dichroism; PC, phosphatidylcholine; PG, phosphatidylglycerol; PA, phosphatidic acid; SP, sphingomyelin; Chol, cholesterol; DOC, sodium deoxycholate; DTT, dithiothreitol; Gdn·HCl, guanidinium hydrochloride; DPH, 1,6-diphenyl-1,3,5-hexatriene; FP, fluorescence polarization; EM, electron microscopy; PrP 106-126, PrP fragment 106-126.

than PrP^{Sc} (2). PrP106 has been found to sustain prion replication when expressed in transgenic mice with a PrP knock-out genetic background (3). Recombinant PrP106 (rPrP106) shows properties similar to those of $PrP^{Sc}106$ extracted from scrapie-infected PrP106-transgenic mice, such as high β-sheet content, resistance to limited digestion by proteinase-K (PK) and high thermodynamic stability (4). These observations have emphasized the importance of studying the structure and biology of PrP106, which can be considered a model of protein folding intermediates that feature in PrP^{C} to PrP^{Sc} conversion.

In the present study, we report the synthesis, physicochemical properties and *in vitro* neurotoxicity of PrP106. Synthetic proteins are devoid of any biological contaminant and are especially desirable for biological assays. In prion research, homogeneity of the protein studied has a particular relevance since it has been discussed the role of potential cofactors, such as protein X, in PrP^{C} to PrP^{Sc} conversion (5). In addition, modified amino acids can be easily introduced in specific sites of the primary structure of synthetic proteins to facilitate structural and functional studies. However, classical stepwise solid-phase synthesis (SSPS) is not convenient for the production of long polypeptides due to the progressive decrease of synthetic efficiency with the increase of the number of amino acids. This leads to difficult or almost impossible purification of the full-length protein from its truncated side products. To overcome these problems, new sophisticated but laborious chemistries, such as native chemical ligation, have been developed for total synthesis of wild-type and engineered proteins (6,7).

Here we described a straightforward protocol to produce relatively large amount of PrP106, combining classical SSPS with a special purification strategy based on specific and transient labelling of the polypeptide with a lipophilic chromatographic probe (8). Furthermore, we found that synthetic PrP106 (sPrP106) possesses physicochemical and biological properties similar to those of PrP^{Sc}. Accordingly, this synthetic miniprion is an

excellent tool for investigating the molecular basis of the conformational conversion of PrP^{C} into PrP^{Sc} and the biology of prion diseases.

EXPERIMENTAL PROCEDURES

Peptide Synthesis, Derivatization and Purification

PrP106 (GQGGGTHNQWNKPSKPKTNMKHMAGAAAAGAVVGGLGGYMLGS AMSRPMIHFDCVNITIKQHTVTTTTKGENFTETDVKMMERVVEQMCVTQYQKESQA YYDGRRS) was synthesized by SSPS on an automated Applied Biosystems synthesizer model 433A at 0.1 mM scale with HMP resin from N-(9-fluorenyl)methoxycarbonyl (Fmoc) protected L-aminoacid derivatives. Amino acids were activated by reaction with N-[(1H-benzotriazol-1-yl)(dimethylamino)methylene]-N-methylmethanaminium hexafluorophosphate N-oxide and N,N-diisopropylethyl-amine. A capping step with acetic anhydride after the last coupling cycle of each amino acid was included.

PrP106 still attached to the resin was derivatized at the N-terminus with a lipophilic probe (4-dodecylaminocarbonyl-fluorene-9-ylmethyl succinimidyl carbonate) following the method described by Mascagni (8) with some modifications. Briefly, 4 equivalents of the probe were dissolved at a concentration of 0.2 M in trifluoroethanol (TFE):dichloromethane (DCM) = 1:3 (v/v) and added to the polypeptidyl-resin suspended in DCM. The reaction mix was incubated for 2 h and the completion of the reaction was determined by the ninhydrin test (9).

After evaporation of the DCM under a stream of nitrogen, the peptide was cleaved from the resin with trifluoroacetic acid (TFA)/thioanisole/water/phenol/ethanedithiol 82.5:5:5:5:2.5 (v/v), precipitated and washed with diethylether. The precipitate was further washed with acetonitrile/water (7:3), dissolved in 60% formic acid and purified by reverse-phase (RP) HPLC on a semipreparative C4 column (Symmetry300, 19 x 150 mm, particle size 7 μm, Waters), with a mobile phase of 0.1% TFA/water (eluent A) and 0.08% TFA/acetonitrile (eluent B) using a linear gradient of 15-50% eluent B in 40 min. The 300

nm-absorbing peak was collected and characterized by matrix-assisted laser desorption/ionization (MALDI) mass spectrometry (MS). The pooled fractions containing the homogeneous labelled miniprion were lyophilzed. The probe was removed by a 2 h-treatment with 10% triethylamine (TEA) in acetonitrile/water (1:1). After lyophilization, the peptide was dissolved in concentrated TFA and precipitated with diethylether. The pellet was redissolved in acetonitrile/water (1:1) and relyophilized. Tipically this procedure enables to obtain about 50 mg of pure sPrP106, representing an overall yield of 5%.

Circular dichroism spectroscopy

Circular dichroism (CD) spectra were recorded with a Jasco J-710 CD spectrometer (Jasco, Easton, MD) scanning spectra at a speed of 20 nm/min, with a bandwidth of 2 nm and a step resolution of 0.2-1 nm using quartz cells with an optical path of 0.1 cm. Aliquots of lyophilized sPrP106 were dissolved in (i) deionized water, (ii) 1 mM sodium acetate, pH 5.5, (iii) saline, (iv) 1 mM sodium acetate containing liposomes or 20% TFE, (v) deionized water containing 20%, 40% or 60% TFE, at a concentration of 0.05-1 mg/ml as specified in Table 1. Protein solutions were incubated at room temperature for different times (from 1 h to one week) before measurement. No substantial variations were observed at different incubation times. Background spectra were subtracted, and the data were converted to molar ellipticity. Each spectrum shown is the result of the accumulation of 4-5 individual spectra. The secondary structure content was calculated using a program DICROPROT V2.5, which contains a least square method based on the Gauss-Jordan elimination (10), the self consistent method and the variable selection method (11).

Liposome preparation

Multilamellar vescicles of different composition were prepared as previously described (12). Phosphatidylcholine (PC), phosphatidylglycerol (PG), phosphatidic acid (PA), sphingomyelin (SP) and cholesterol (Chol) purchased from Sigma were mixed at the following molar ratios: PC:Chol (1:1), PC:SP (1:1), PC:PA:Chol (1:1:1), and PG:Chol (1:1). For the experiments liposomes were resuspended in 1 mM sodium acetate, pH 5.5. CD experiments were performed after addition of liposome suspensions to sPrP106 solution in the same buffer, to obtain a final peptide concentration of 0.1 mg/ml and a protein:lipid molar ratio of 1:25.

Proteinase-K digestion

sPrP106 was digested with PK in the presence or absence of detergents. In a first set of experiments, the protein (0.2 mg/ml) was incubated in 10 mM Tris·HCl, pH 7.4/100 mM NaCl/0.5% NP-40/0.5% sodium deoxycholate (DOC) at 37°C up to 1h. The PK:protein ratios employed were 1:320, 1:160, 1:32, 1:16, 1:3.2. The reaction was stopped by adding phenylmethanesulfonyl fluoride to a final concentration of 5 mM. Samples were analyzed by SDS-PAGE and visualized by Coomassie staining or by Western blotting using monoclonal antibody 3F4 and polyclonal antibody R340. Alternatively, the protein (1 mg/ml) was incubated at 37°C in 1 mM sodium acetate, pH 5.5, with an enzyme to protein ratio of 1:50. During PK-digestion, aliquots were taken every 30 min up to 5 h. After addition of an equal volume of 1% TFA, the samples were analysed by MALDI MS.

MALDI mass spectrometry

Fragments or full-length sPrP106 were analyzed by a Bruker Biflex™ or a Reflex III™ MALDI mass spectrometer. Few µl of the sample were mixed with an equal volume of a

saturated solution of sinapinic acid (Sigma-Aldrich) in acetonitrile/0,1% TFA 1:3 (v:v) and 1 µl of the mixture was deposited on the MALDI target.

Electron microscopy

Aliquots of lyophilized PrP106 were suspended in aqueous solutions with different pH and ionic strength at a final concentration of 0.1 and 0.3 mM. The solvents included (i) deionized water, pH 5.0, (ii) 10 mM Tris·HCl, pH 5.5, (iii) 1 mM sodium acetate, pH 5.5, and (iv) 1 mM sodium acetate, 120 mM NaCl, pH 5.5. In some experiments, the peptide was subjected to reduction and partial denaturation in 10 mM Tris·HCl, 100 mM DTT, 2 M guanidinium hydrochloride (Gdn·HCl), pH 5.5, for 24 hours, followed by refolding by dialysis against deionized water before analysis. After incubation at 37°C for 1h, 48 h and 7 days, 10 µl of each sample were air-dried on gelatine-coated slides, stained with Congo red and viewed under polarized light. Samples for ultrastructural examination were taken after short (1, 4 or 8 h) and long (1, 2, 3 or 7 days) incubation. At each time point, 5 µl of suspension were applied on formvar-carbon 200 mesh nickel grids for 5 min and negatively stained with freshly filtered uranyl acetate. After drying, samples were observed with an electron microscope (EM109 Zeiss, Oberkoken, Germany) operated at 80 KV at a standard magnification of 30,000. The magnification was calibrated using an appropriate grid. At day 7, samples were centrifuged at 16,000 g for 15 minutes. The pellet was fixed in 2.5% glutaraldehyde in 0.05% phosphate buffer, pH 7.4, post-fixed in osmium tetroxide, dehydrated in graded acetone and embedded in epoxy resin (Spurr, Electron Microscopy Science, Fort Washington, PA, USA). Ultrathin sections (500 Å) were collected on 200 mesh copper grids, positively stained with uranyl acetate and lead citrate and observed with the electron microscope. The mean diameter and length were measured on printed photos at a

final magnification of 90,000 using a computer assisted image analyzer (Nikon corporation, Shinagawa-Ku, Tokio, Japan).

Neurotoxicity

Primary cultures of rat cortical neurons were prepared as previously described (13). Briefly, brains were removed from fetal rats on embryonic day 17. Cortical cells were dissociated and plated at the density of $5x10^5$ cells per well. The cells were cultured in basal medium Eagle (BME-Hanks' salt, GIBCO) supplemented with 10% fetal calf serum (FCS, GIBCO) and 2 mM glutamine. sPrP106 was dissolved in deionized water and added to the medium, for the acute treatment (final concentration 5 and 10 µM), on day 5 of culture and the cell viability was determined 24 hours later. For the chronic treatment SPrP 106 was added to the medium on days 1, 3, 5 of culture, reaching final concentrations of 0.5, 1, 5 and 10 µM in the well, the cell viability was determined at day 7. Cell viability was assessed quantitatively by the MTT method (14) with an automated micro plate reader (Perkin-Elmer lambda reader).

Microviscosity

Membrane microviscosity was assessed in suspensions of rat primary neurons and liposomes using 1,6-diphenyl-1,3,5-hexatriene (DPH) as a fluorescent probe as previously described (15,16). The reported fluorescence polarization (FP) value is a function of the emission (420 nm) detected through an analyzer oriented parallel (p_1) and perpendicular (p_2), to the direction of the polarization of the exciting light (365 nm), according to the equation $p=(p_2–p_1)/(p_2+p_1)$ (17). Membrane microviscosity (η, poise) is related to FP according to the formula $\eta = 2p/(0.46–p)$ (17). Neuronal cells were mechanically detached, gently centrifuged at 550 x *g* for 10 min, washed with saline, resuspended in 2.5 ml of 2 µM DPH in 5 mM

sodium acetate, pH 5.5, and incubated for 30 min at room temperature. The FP value (expressed as arbitrary units) was determined at 25°C, before and 10 min after the addition of increasing concentration of sPrP106 to the cells or liposome suspensions placed in the cuvette. Each value is the mean ± SD of at least four determinations.

Secondary structure and transmembrane helix predictions

For secondary structure prediction the Double Prediction Method was used (18) (http://npsa-pbil.ibcp.fr/). For prediction of membrane protein topology the TMHMM method, based on a hidden Markov model developed by Anders Krogh and Erik Sonnhammer, was applied (19) (http://www.cbs.dtu.dk/services/TMHMM/).

RESULTS

Synthesis, purification and characterization of PrP106

PrP106 was synthesized by Fmoc-based SSPS with some modifications. It was necessary to introduce several double coupling cycles to enhance the coupling efficiency in correspondence of the difficult sequences identified by conductivity measurements. In addition, three deprotection cycles where added after coupling of each amino acid. This step was found to greatly improve the yield of the synthesis.

A special strategy was adopted for the purification of sPrP106 from its truncated forms, which were co-eluting or eluting very closely to the full-length protein (Fig. 1A). The target protein was labelled with a specific and transient labelling, a lipophilic Fmoc-based chromatographic probe. The probe reacted efficiently with the free amino terminus of the protein as checked by ninhydrin reaction. It should be recalled that the N-terminus of sPrP106 is the only available site for the reaction, since the N-termini of truncated peptides are acetylated in the capping step after each coupling cycle. On RP-HPLC the derivatized synthetic PrP106 (dsPrP106) eluted considerably later than the closely related impurities (Fig. 1B) and was easily monitored at 300 nm (Fig. 1C). The purified dsPrP106 was characterized by MALDI MS (Fig. 2A). The probe was removed by basic hydrolysis with TEA and discharged simply by extraction with diethylether, thus avoiding an additional chromatographic step. Finally the pure protein was characterized by MALDI MS (Fig. 2B). The observed molecular weights of dsPrP106 and sPrP106 were 11998.6 and 11572.6 Da, respectively, which are in good agreement with the calculated molecular weights (12001.7 and 11570.1 Da).

sPrP106 adopts a stable β-sheet-rich secondary structure

The secondary structure of sPrP106 in different environments was investigated by CD spectroscopy in the far UV. Measurements were performed at protein concentrations of 0.05, 0.1, 0.5 and 1 mg/ml. The protein adopted a stable conformation with high percentage of β-sheet (around 40%, calculated with different deconvolution programs), independently from its concentration (Fig. 3A), ionic strength (Fig. 3B) and time of incubation (Table 1). All spectra showed the characteristic β-sheet single minimum between 210 and 220 nm. The secondary structure was not substantially affected by the addition of 20% TFE or liposomes to peptide solutions in 1 mM sodium acetate, pH 5.5 (Fig. 3B). A similar result was observed when 20% TFE was added to sPrP106 dissolved in deionized water at a concentration of 1 mg/ml (Table 1). Conversely, at low protein concentration (0.1 mg/ml), the addition of 20%, 40% or 60% TFE to deionized water resulted in progressive increase in α-helical structure (Fig. 3C, Table 1); with high percentage of TFE (40%-60%), the 208-nm band clearly showed a larger intensity than the 222-nm band, a typical feature of a protein where α helices and β sheets are located in separated domains and do not intermix along the polypeptide chain (20).

To verify whether the structural characteristics and stability of sPrP106 were the result of inter-molecular disulfide bridge formation during the purification process, the protein was denaturated with 20 mM sodium acetate pH 5.5/8 M Gdn·HCl/100 mM DTT and refolded following dialysis against 20 mM sodium acetate, pH 5.5. The CD spectrum of refolded sPrP106 was marked by a high β-sheet content, although a broader minimum band was observed in the 210-220 nm region (fig. 3D).

In addition to CD determinations, the Double Prediction Method (18) was used for secondary structure prediction. The algorithm indicated that the region of the protein comprising residues 138-217 has propensity to acquire β-sheet structure (Fig. 4).

sPrP106 contains a PK resistant C-terminal domain

Experiments of PK-resistance were performed in different conditions. In a first set of experiments sPrP106 was digested in the presence of detergents (NP-40 and DOC) at increasing PK:protein ratio from 1:320 to 1:3.2. The digestion products were analyzed by SDS-PAGE and visualized by Coomassie staining or Western blotting using two different antibodies. Figure 5A shows that an approximately 5-6 KDa-resistant core, constituted probably by more than one component, withstood digestion even at a PK:protein ratio of 1:3.2 after 60 min incubation. The PK-resistant fragments were not detected by Western blotting using monoclonal antibody 3F4 (Fig. 5B), whose epitope is located on the N-terminal segment of the protein. Conversely, the antibody R340, which recognizes epitopes on the C-terminal portion (beyond amino acid 134) of mouse PrP, immunoreacted with the PK-resistant C-terminal fragments of sPrP106 (Fig. 5C).

The PK-resistant fragments were characterized by MALDI MS. To be able to directly analyze the samples on MALDI MS, the digestion was carried out in 1 mM sodium acetate, pH 5.5, in the absence of detergents. The information obtained from Western blot analysis, the purity and the relatively small size of sPrP106, and the accuracy of the mass measurements allowed us to unambiguously identify the sequence of PK-resistant fragments. Already after 30 min digestion, sPrP106 lost its N-terminal portion generating peptides starting at amino acid residue Ser134 and having a ragged C terminus corresponding to residues 224, 220, 218, 217, and 215 (Table 2) in agreement with published results obtained with rPrP106 (4). The most abundant fragment was 134-224 after 30 min incubation (data not shown) and 134-217 after 2 up to 5 h of PK digestion (Fig. 6).

sPrP106 assembles in branched filamentous structures

The nature of aggregates generated by sPrP106 was determined by electron microscopy (EM) after negative and positive staining and by polarized light microscopy after incubation with Congo red. The peptide was soluble in deionized water, 10 mM Tris·HCl, pH 5.5, and 1 mM sodium acetate, pH 5.5, at concentrations of up to 4 mg/ml. Under these conditions, a few spherical particles with a diameter of 20-30 nm and poorly defined, short, filamentous structures of irregular thickness ranging from 4 to 10 nm were observed by EM after one h incubation. These aggregates were not birefringent after Congo red staining and increased significantly in number during the first 24 h. No substantial modifications were detected at longer times (up to 7 day incubation) except for an increased packing of aggregates; in particular, no amyloid-like fibrils were ever observed. Enhancing the ionic strength by the addition of 120 mM NaCl to 1 mM sodium acetate buffer, resulted in increased aggregation of the peptide, without apparent modifications of the structure and staining properties of the aggregates. On the other hand, reduction and partial denaturation of sPrP106 followed by refolding yielded an increase in thickness, length and number of the filamentous structures, that formed dense meshworks in the absence of definite amyloid-like fibrils. EM examination of the pellets obtained by centrifugation of peptide suspensions after 7 days allowed a better definition of the fine morphology of different types of aggregates and the evaluation of their relative amount (Fig. 7A-C). Following incubation in acidic water, 10 mM Tris·HCl (Fig. 7 A) or 1 mM sodium acetate (data not shown), the preparations contained comparable amounts of finely granular, osmiophilic material and filamentous structures. The filaments had an irregular diameter ranging from 4 to 10 nm (mean ± SD: 7.3 ± 2.3) and a length of 0.1-2 μm; they were usually twirled and branched, and built loose meshworks. Following reduction, denaturation and refolding, peptide assemblies were more structured and better defined (Fig. 7C). They consisted of slightly curved, often branched filaments with a

diameter ranging from 8 to 22 nm (19.7 ± 3.7) and a length ranging from 0.8 to 4 μm. The filaments had a rosary-like profile without a clear twisting or crossover. Spherical and ring-shaped structures, likely representing the cross section of single filaments, were also observed. Conversely, finely granular, amorphous material was almost absent. Following incubation in sodium acetate containing 120 mM NaCl, the peptide aggregates showed intermediate features, in that they consisted of very abundant, thin, short, often branched filaments with a diameter ranging from 5 to 12 nm (9.4 ± 2.6) and a length of 0.5 to 2 μm, mixed with small amount of finely granular, osmiophilic material (Fig. 7B).

sPrP106 is neurotoxic to primary rat cortical neurons

To evaluate the effects of sPrP106 on cell viability, primary rat cortical neurons were exposed for 24 hours (5 and 10 μM) or for 7 days (0.5-10 μM) to the synthetic protein. The 24-hours exposure did not affect the neuronal viability (data not shown), whereas a statistically significant neurotoxic effect was detected after the chronic treatment at the higher protein concentrations (Fig. 8). The cell viability was reduced of about 40% and 60%, compared to the controls, with the exposure to sPrP106 at 5 and 10 μM respectively (Fig. 8).

sPrP106 increases membrane microviscosity

The ability of sPrP106 to affect membrane microviscosity was analyzed on suspensions of primary rat cortical neurons following incubation with DPH fluorescent probe. Table 3 reports the FP value before and after addition of increasing concentrations of sPrP106. A striking, dose-dependent rigidifying effect on nerve cell membranes was detected at 5, 10 and 20 μM protein concentration, with 56%, 64% and 105% increase in basal FP value, respectively. This effect was higher than the one observed with the syntetic peptide PrP106-126, which yielded a 48% increase in membrane microviscosity at 25 μM

concentration. sPrP106 was also tested on artificial membranes of different composition and charge, using 10 μM protein concentration. The rigidifying effect was consistent with neutral liposomes prepared with PC:Chol (1:1) and PC:SP (1:1) and negatively charged PG:Chol (1:1) liposomes, with an increase in FP of 31%, 45% and 24% of basal value, respectively. Conversely, the effect was much lower (7% increase) with positively charged liposomes prepared from PC:PA:Chol (1:1:1).

The membrane protein topology prediction method (19), TMHMM, gave a high score for the insertion of sPrP106 in the membrane through a transmembrane helix spanning residues 111-133, with the N-terminal extracellular domain corresponding to residues 89-110 and the C-terminal cytoplasmatic domain comprising residues 134-230 (Fig. 4).

DISCUSSION

Synthetic peptides derived from discrete PrP regions have been extensively used to identify protein domains that could be involved in the conformational transition of PrP^{C} to PrP^{Sc} and in disease pathogenesis (1). In particular, the peptide PrP106-126 was found to possess many of the PrP^{Sc} properties, including the propensity to adopt a β-sheet conformation and form amyloid fibrils, the partial resistance to PK digestion, and the ability to induce nerve cell degeneration and glial cell activation *in vitro* (1,13,21).

A major concern in using small PrP peptides is that they can adopt conformations, which may differ from their actual structure in the entire protein. Moreover, although such peptides are very useful for cell culture studies, they are not capable to induce disease when administered to animals. Supattapone et al. (3) showed that the minimal sequence that sustains prion replication corresponds to a redacted version of PrP lacking residues 23-88 and 141-176. This peptide termed PrP106 or miniprion is currently regarded as an excellent model to unravel both the conversion of PrP^{C} to PrP^{Sc} and prion pathogenesis.

Our decision to generate synthetic rather than recombinant PrP106 was based on the assumption that accurate mechanistic studies can be carried out only with a pure protein devoid of any cellular contaminant. This idea is substantiated by the knowledge that several proteins with high affinity for PrP^{C} or PrP^{Sc} may play an important role in the conversion reaction and disease propagation (5). Ball et al. have recently reported the synthesis of PrP polypeptides by highly optimized Fmoc/t-Boc protocols and chemical ligation (7). Our procedure to generate relatively large amount of sPrP106 was straightforward and simple. Its strength resides on a special purification strategy based on the use of a lipophilic chromatographic probe (8), which enables us to purify the full-length protein from the side

products by a single chromatographic step. This fact minimizes the losses and compensates for the low yield of the chemical synthesis of a long polypeptide by classical Fmoc-based SSPS. Following this strategy, the overall yield of PrP106 was 5%, which is satisfying for an easy-to-aggregate PrP polypeptide.

sPrP106 showed interesting biochemical features. First, the protein had a high propensity to adopt a secondary structure with high β-sheet content. The amount of β-sheet was similar in different conditions, at variance with PrP106-126 that shows an environmental-dependent conformational polymorphism. Furthermore, the behaviour of the synthetic protein was slightly different from that of its recombinant counterpart, rPrP106 (4). In fact, sPrP106 exhibited a well-ordered structure already at low concentration (0.1 mg/ml, i.e. 8.6 μM) in 1 mM sodium acetate pH 5.5, while rPrP106 was found to undergo a concentration-dependent conformational transition from an unfolded monomeric state to an ordered β-sheet multimeric assembly in the range of 30-100 μM (4). Second, sPrP106 contains a C-terminal domain, which is notably insensitive to PK degradation. Even at stringent conditions of PK-to-protein ratio and prolonged digestion times, a protease-resistant core mainly composed of a fragment spanning residues 134-217 was consistently detected. The results from CD determination and PK-digestion suggest that the tertiary structure of sPrP106 may consist of a flexible N-terminal domain and a C-terminal β-sheet domain starting approximately at Ser134. This hypothetical structure is supported by the algorithm of the Double Prediction Method (18).

The macromolecular assemblies generated by sPrP106 in different conditions were analyzed by EM. Protein suspensions in aqueous solutions contained a few spherical particles with a diameter of 20-30 nm, short filamentous structures of irregular thickness ranging from 4 to 10 nm, and amorphous granular material. The heterogeneity of sPrP106 aggregates was not longer observed when the protein was subjected to reversible denaturation followed by refolding. Under these conditions, the preparations essentially contained branched filaments

with a relatively regular, rosary-like profile, and a diameter ranging from 8 to 22 nm. The filamentous aggregates were not birefringent under polarized light after Congo red staining. It remains possible that further manipulations, such as reducing conditions, low pH, partially denaturating environments (0.5-1 M Gdn·HCl) could favour the formation of amyloid-like fibrils (22,23). Nonetheless, the formation of ordered but not amyloid-like structures might be compatible with the peculiar parallel β-helix fold, which is the feature of $PrP^{Sc}106$ crystals as recently shown by electron crystallography studies (24).

Evidence suggests that the neuropathological changes observed in prion diseases are due, at least in part, to accumulation of PrP^{Sc}. This view is supported by the observation that the protease resistant core of PrP^{Sc} has a variety of pathogenic effects *in vitro*, including neurotoxicity and ability to interact with plasma membrane yielding increased microviscosity. Similar effects have been observed with short synthetic peptides, in particular with PrP106-126. Our study shows that sPrP106 not only maintains these properties but it is more effective than PrP106-126. In fact, the concentrations required to obtain the same extent of nerve cell death and a similar increase in membrane microviscosity were five times lower with sPrP106 than with PrP106-126 (13,16). At variance with PrP106-126, the interaction of sPrP106 with multilamellar vescicles was influenced by their net charge and composition (12). This is likely related to a distinctive interaction of sPrP106 with membranes rather than to the net charge of the polypeptides, since sPrP106 and PrP106-126 are both positive. sPrP106 contains the membrane-spanning domain (roughly residues 113-135) of PrP (25, 26). Interestingly, the application of a membrane protein topology prediction method (19), TMHMM, indicated that sPrP106 possesses the characteristics to insert into the membrane through a transmembrane helix spanning residues 111-133.

In conclusion, our study shows that sPrP106 (i) readily adopts a stable β-sheet conformation, (ii) contains a protease-resistant core, (iii) assembles in relatively regular

filamentous structures, (iv) is highly neurotoxic and (v) interacts with membranes inducing a remarkable increase in microviscosity. These properties make sPrP106 a promising model to investigate the PrP^{C}>PrP^{Sc} conversion process and disease pathogenesis.

ACKNOWLEDGMENTS

This work was supported by grants from Telethon-Italy (No. 466/bi to V.B., 83CP to R.C.; R.C. is an Assistant Telethon Scientist), Italian Ministry of Health (RF99.38), the Italian Ministry of University and Research (MIUR, PRIN2001) and the European Union (QLRT 01-00283, BMH4 98-605, QLTR-2000-02353). We would like to thank P. Mascagni for supplying us with the lipophilic probe for sPrP106 purification and for fruitful suggestions, C. Weissmann and R. Kasaks for kindly providing us respectively with the antibodies R340 and 3F4.

LEGENDS TO THE FIGURES

Figure 1. Analytical RP-HPLC on C_{18} media of (A) crude material from the synthesis of PrP106 directly after the cleavage from the resin, monitored at 214 nm, (B) crude material from the synthesis of PrP106 after derivatization with lipophilic probe and cleavage from the resin, monitored at 214 nm. The arrow indicates the peak correspondent to the derivatized peptide. (C) Same as B but monitored at 300 nm.

Figure 2. MALDI mass spectra of (A) purified dsPrP106 and (B) sPrP106 after removal of the chromatographic probe.

Figure 3. Far UV CD spectra of (A) 0.05, 0.1 and 0.5 mg/ml sPrP106 in water; (B) 0.1 mg/ml sPrP106 in 1 mM sodium acetate pH 5.5, in the same buffer + 20% TFE, in the same buffer + liposomes, in saline solution; (C) 0.1 mg/ml sPrP106 in water + 20% TFE, in water + 40% TFE, in water + 60% TFE; (D) 0.5 mg/ml sPrP106 denaturated in 20 mM sodium acetate pH 5.5 /8 M Gdn·HCl/100 mM DTT and refolded in 20 mM sodium acetate pH 5.5, 0.5 mg/ml sPrP106 in 20 mM sodium acetate pH 5.5 without denaturation and refolding process.

Figure 4. Primary structure of sPrP106 and predictions of secondary structure and topology. The synthetic protein corresponds to residues 89-140 and 177-230 of mouse PrP and contain a deletion in the region 141-176. The protein differs from the wild-type at positions 108 and 111, where Met substitutes respectively Leu and Val. These substitutions generate the epitope for the monoclonal antibody 3F4. The PK-resistant fragment is defined by bold and underlined letters. In correspondence of PrP106 sequence the secondary structure prediction is

shown, where "t" stands for β-turn, "c" for random coil, "h" for α-helix and "e" for extended strand. For the secondary structure prediction the Double Prediction Method was used (18). Results from the application of a membrane protein topology prediction method (19), TMHMM, is also reported. The segment designated with "m" is a transmembrane helix, while "o" and "i" segments are extracellular and cytoplasmatic domains, respectively.

Figure 5. SDS-PAGE of the PK-digestion products of sPrP106 in 10 mM Tris HCl, pH 7.4/100 mM NaCl/0.5% NP40/0.5% DOC. sPrP106 in absence of PK (lane 1), after incubation wih PK at 37°C for 30 min (lanes 2,3,4,5,6) and 60 min (lanes 7,8,9). The PK:protein ratio was 1:320 (lane 2), 1:160 (lane 3), 1:32 (lanes 4 and 7), 1:16 (lanes 5 and 8), 1:3.2 (lanes 6 and 9); A: Coomassie stained SDS-PAGE; B: Western blot analysis using monoclonal antibody 3F4; C: Western blot analysis using polyclonal antibody R340.

Figure 6. MALDI mass spectrum of the PK-resistant fragments after 5 h-digestion in 1 mM sodium acetate pH 5.5, with E:S=1:50, at 37° C, where peaks at m/z 5326.3, 5620.5, 5751.5, 6005.7 and 6457.4 correspond respectively to 134-215, 134-217, 134-218, 134-220 and 134-224 PK-resistant sPrP106 fragments.

Figure 7. Electron micrographs of the aggregates generated *in vitro* by sPrP106 in different conditions. Positively stained ultrathin sections of the pellets obtained by centrifugation at 16,000 X g for 15 min after incubation of the peptide at 37˚C for 1 week in (A) 10 mM Tris·HCl, pH 5.5, (B) 1 mM sodium acetate pH 5.5/120 mM NaCl, and (C) deonized water. Sample (C) was subjected to reversible denaturation in 2 M Gdn·HCl/100 mM DTT for 24 h, followed by refolding by dialysis against deionized water. Magnification bar, 100 nm.

Figure 8. The neurotoxic effect of sPrP106 on rat primary cortical neurons was determined after 7-day of chronic exposure to increasing concentrations of the protein, from 0.5 to 10 µM. Data are the mean ± SE of 4 determinations (for 0.5 and 10 µM) and 8 determinations (for 1 and 5 µM); *P<0.01 versus control (Tukey's test).

REFERENCES

1. Tagliavini, F., Forloni, G., D'Ursi, P., Bugiani, O., and Salmona, M. (2001) *Adv. Protein Chem.* **57**, 171-201

2. Muramoto, T., Scott, M., Cohen, F. E., and Prusiner, S. B. (1996) *Proc. Natl. Acad. Sci. U. S. A.* **93**, 15457-15462

3. Supattapone, S., Bosque, P., Muramoto, T., Wille, H., Aagaard, C., Peretz, D., Nguyen, H. O., Heinrich, C., Torchia, M., Safar, J., Cohen, F. E., DeArmond, S. J., Prusiner, S. B., and Scott, M. (1999) *Cell* **96**, 869-878

4. Baskakov, I. V., Aagaard, C., Mehlhorn, I., Wille, H., Groth, D., Baldwin, M. A., Prusiner, S. B., and Cohen, F. E. (2000) *Biochemistry* **39**, 2792-2804

5. Prusiner, S. B. (1998) *Proc. Natl. Acad. Sci. U. S. A.* **95**, 13363-13383

6. Dawson, P. E., Muir, T. W., Clark-Lewis, I., and Kent, S. B. (1994) *Science* **266**, 776-779

7. Ball, H. L., King, D. S., Cohen, F. E., Prusiner, S. B., and Baldwin, M. A. (2001) *J. Peptide Res.* **58**, 357-374

8. Ball, H. L. and Mascagni, P. (1992) *Int. J. Pept. Protein Res.* **40**, 370-379

9. Sarin, V. K., Kent, S. B., Tam, J. P., and Merrifield, R. B. (1981) *Anal. Biochem.* **117**, 147-157

10. Sreerama, N. and Woody, R. W. (1994) *J. Mol. Biol.* **242**, 497-507

11. Manavalan, P. and Johnson, W. C. Jr (1987) *Anal. Biochem.* **167**, 76-85

12. De Gioia, L., Selvaggini, C., Ghibaudi, E., Diomede, L., Bugiani, O., Forloni, G., Tagliavini, F., and Salmona, M. (1994) *J. Biol. Chem.* **269**, 7859-7862

13. Forloni, G., Angeretti, N., Chiesa, R., Monzani, E., Salmona, M., Bugiani, O., and Tagliavini, F. (1993) *Nature* **362**, 543-546

14. Manthorpe, M., Fagnani, R., Skaper, S. D., and Varon, S. (1986) *Brain Res*. **390**, 191-198

15. Diomede, L., Sozzani, S., Luini, W., Algeri, M., De Gioia, L., Chiesa, R., Lievens, P. M., Bugiani, O., Forloni, G., Tagliavini, F., and Salmona, M. (1996) *Biochem. J.* **320**, 563-570

16. Salmona, M., Forloni, G., Diomede, L., Algeri, M., De Gioia, L., Angeretti, N., Giaccone, G., Tagliavini, F., and Bugiani, O. (1997) *Neurobiol. Dis.* **4**, 47-57

17. Shinitzky, M. and Barenholz, Y. (1978) *Biochim. Biophys. Acta* **515**, 367-394

18. Deleage, G. and Roux, B. (1987) *Protein Eng.* **1**, 289-294

19. Krogh, A., Larsson, B., von Heijne, G., and Sonnhammer, E. L. (2001) *J. Mol. Biol.* **305**, 567-580

20. Manavalan, P. and Johnson, W. C. Jr (1983) *Nature* **305**, 831-832

21. Kourie, J. I. (2001) *Chem.-Biol. Interact.* **138**, 1-26

22. Jackson, G. S., Hosszu, L. L., Power, A., Hill, A. F., Kenney, J., Saibil, H., Craven, C. J., Waltho, J. P., Clarke, A. R., and Collinge, J. (1999) *Science* **283**, 1935-1937

23. Morillas, M., Vanik, D. L., and Surewicz, W. K. (2001) *Biochemistry* **40**, 6982-6987

24. Wille, H., Michelitsch, M. D., Guénebaut, V., Supattapone, S., Serban, A., Cohen, F. E., Agard, D. A., and Prusiner, S. B. (2002) *Proc. Natl. Acad. Sci. U. S. A.* **99**, 3563-3568

25. Hegde, R. S., Mastrianni, J. A., Scott, M. R., DeFea, K. A., Tremblay, P., Torchia, M., DeArmond, S. J., Prusiner, S. B., and Lingappa, V. R. (1998) *Science* **279**, 827-834

26. Tompa, P., Tusnady, G. E., Cserzo, M., and Simon, I. (2001) *Proc. Natl. Acad. Sci. U. S. A.* **98**, 4431-443

Table 1: Percentage of sPrP106 secondary structure in various conditions

sPrP106 solutions	% α-helix	% β-sheet
0.1 mg/ml in water	12	38
0.5 mg/ml in water	12	38
0.1 mg/ml in sodium acetate, pH 5.5 (24 h)	12	41
0.1 mg/ml in sodium acetate, pH 5.5 (1week)	11	42
0.5 mg/ml denaturated and refolded in sodium acetate	10	36
0.1 mg/ml in saline	11	40
0.1 mg/ml in sodium acetate, pH 5.5 + liposomes	10	42
0.1 mg/ml in sodium acetate, pH 5.5 + 20% TFE	11	41
0.1 mg/ml in water + 20% TFE	23	28
1 mg/ml in water + 20% TFE	13	39
0.1 mg/ml in water + 40% TFE	35	23
0.1 mg/ml in water + 60% TFE	45	16

Table 2: Identification of PK-resistant sPrP106 fragments

PK-resistant fragments	Sequence	Mw measured*	Mw calculated**
134-224	SRPMIHFDCVNITIKQHTVTTTTKGENFT ETDVKMMERVVEQMCVTQYQKESQAY	6455.3±2.3	6455.4
134-220	SRPMIHFDCVNITIKQHTVTTTTKGENFT ETDVKMMERVVEQMCVTQYQKE	6004.9±2.6	6005.9
134-218	SRPMIHFDCVNITIKQHTVTTTTKGENFT ETDVKMMERVVEQMCVTQYQ	5748.8±2.6	5748.6
134-217	SRPMIHFDCVNITIKQHTVTTTTKGENFT ETDVKMMERVVEQMCVTQ	5619.6±1.6	5620.5
134-215	SRPMIHFDCVNITIKQHTVTTTTKGENFT ETDVKMMERVVEQMCVT	5327.2±2.6	5329.2

*Mw measured is the mean of 6 determinations ± SD

**Mw calculated considering the formation of a disulfide bridge

Table 3: Effect of sPrP106 on fluorescence polarization (FP) value of neuronal cells

sPrP106 (μM)	FP value (arbitrary units)±SD
None	0.128±0.025
0.25	0.126±0.003
0.5	0.140±0.001
1.0	0.153±0.003
5.0	0.200±0.002**
10.0	0.210±0.006**
20.0	0.262±0.005**

**p≤0.01, Student's t test versus basal value

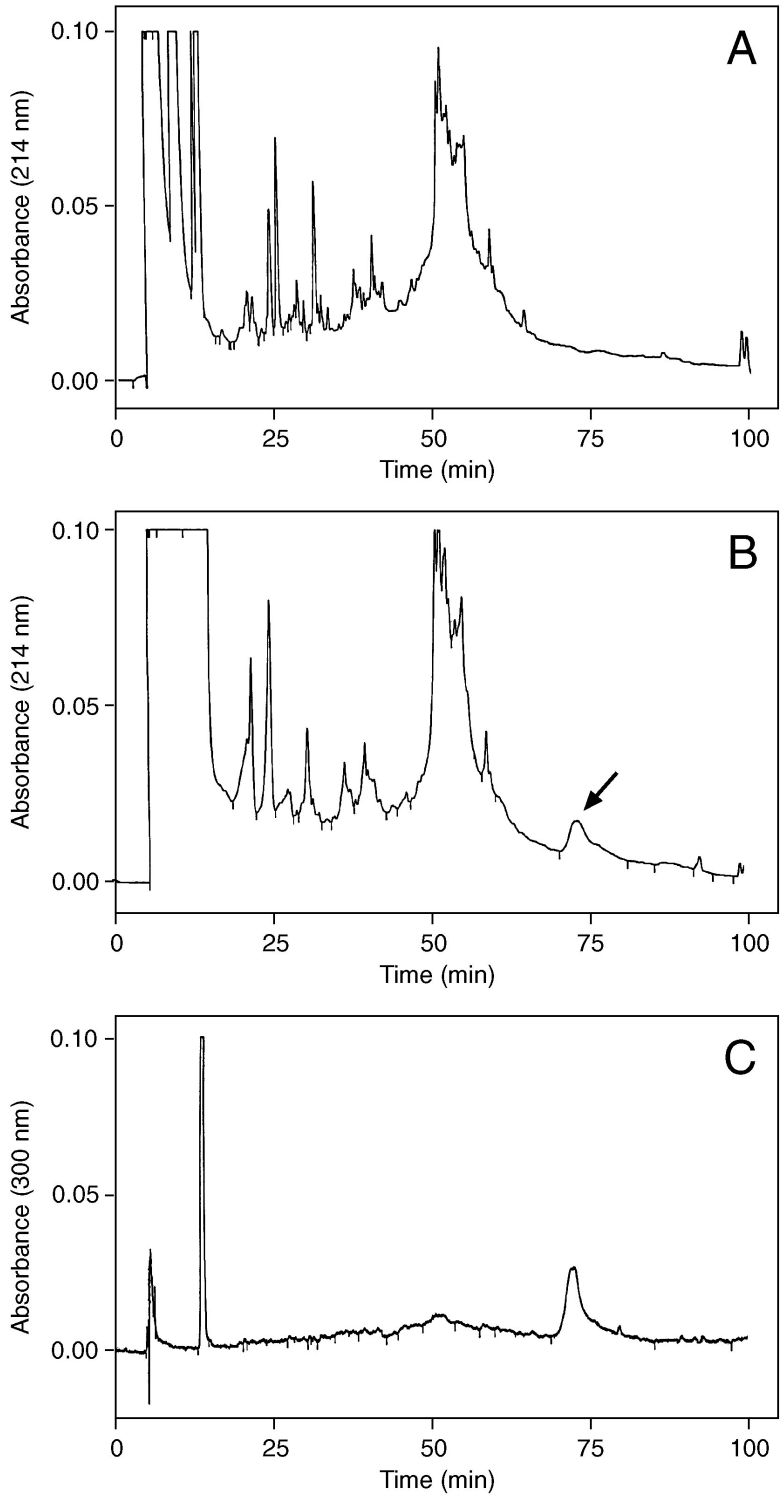

Fig.1

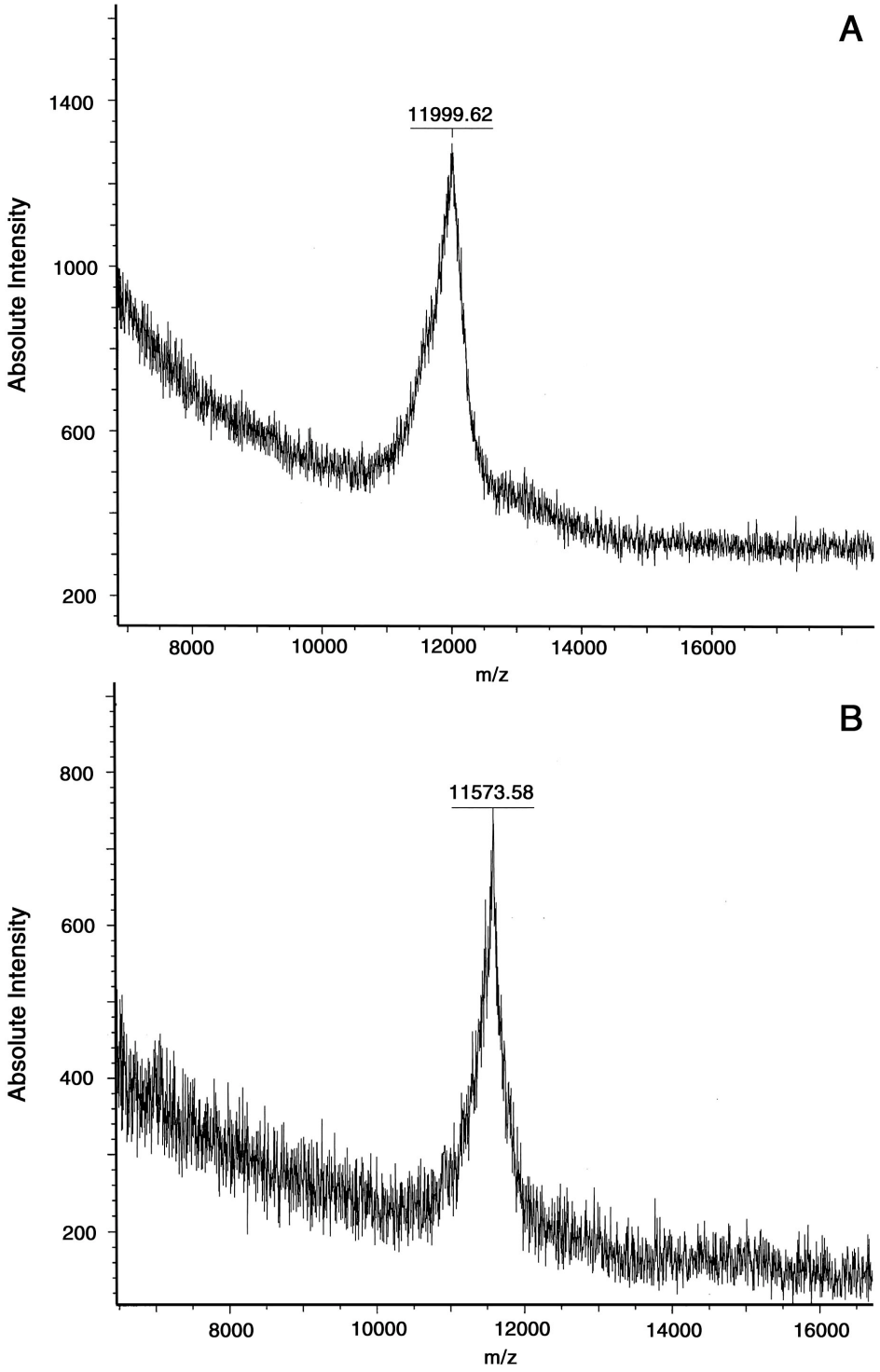

Fig.2

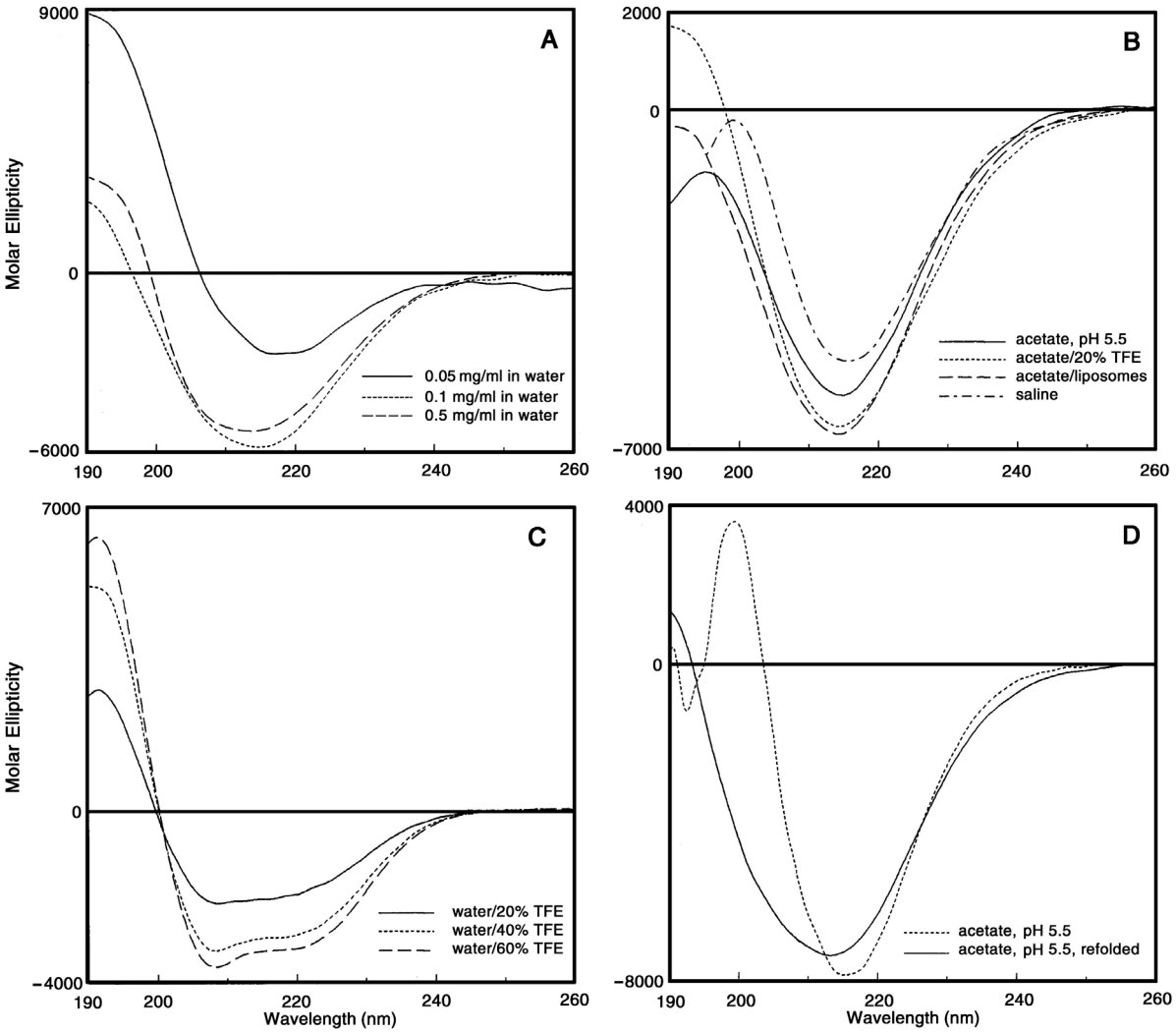

Fig.3

Fig.4

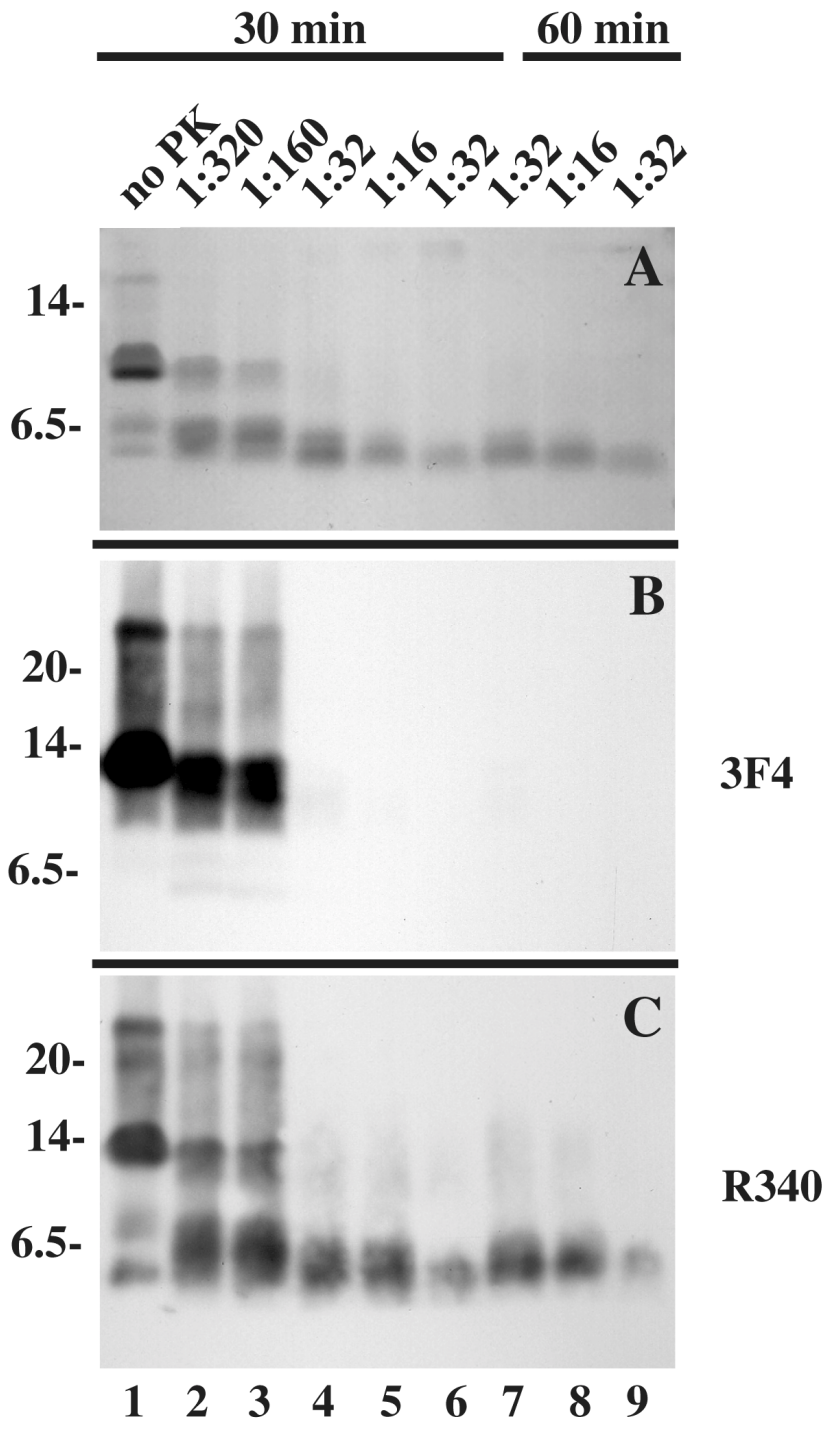

Fig.5

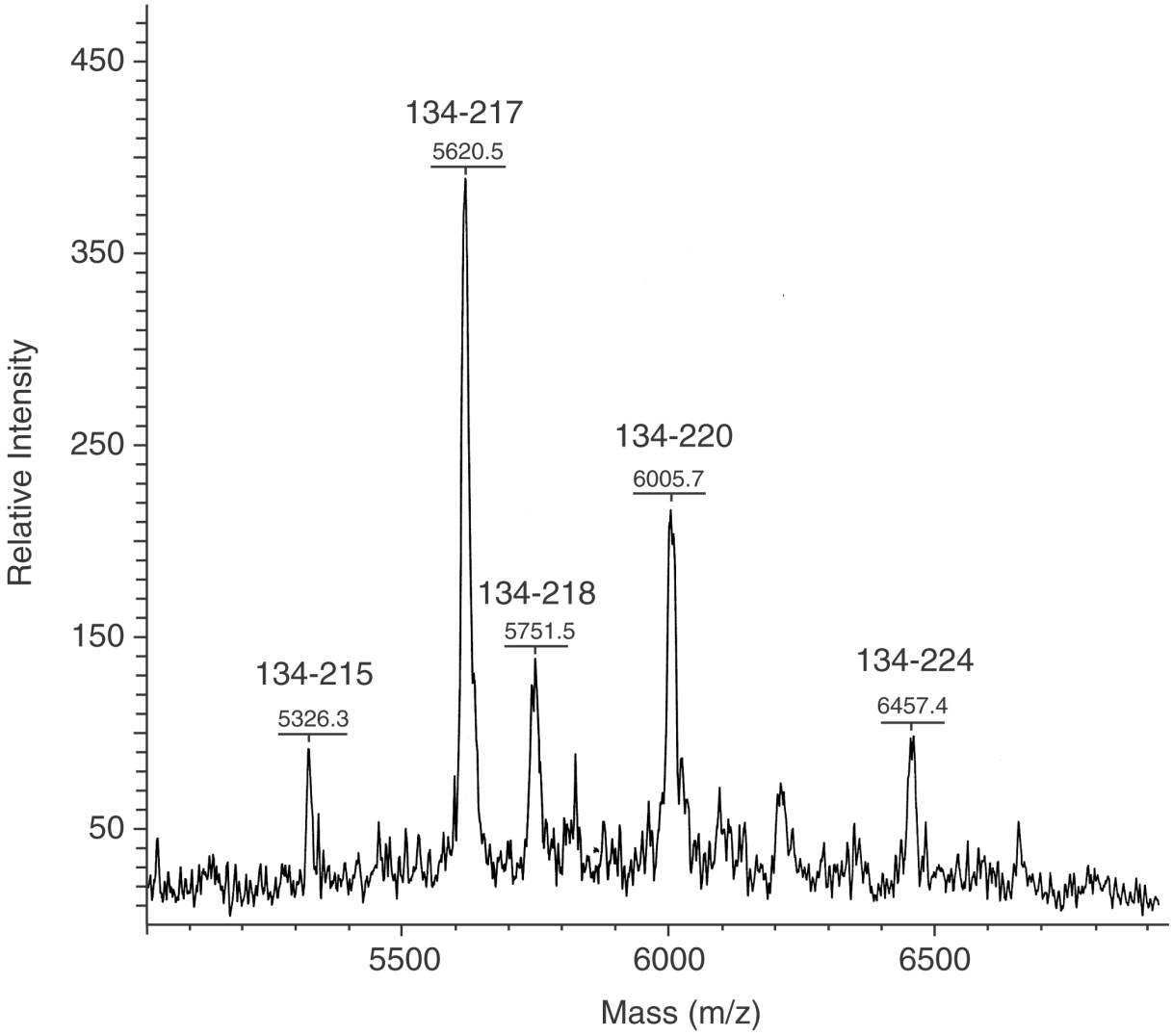

Fig.6

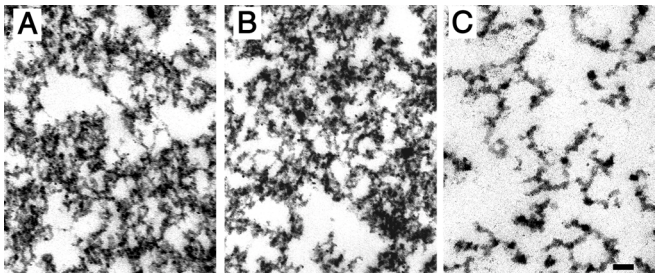

Fig.7

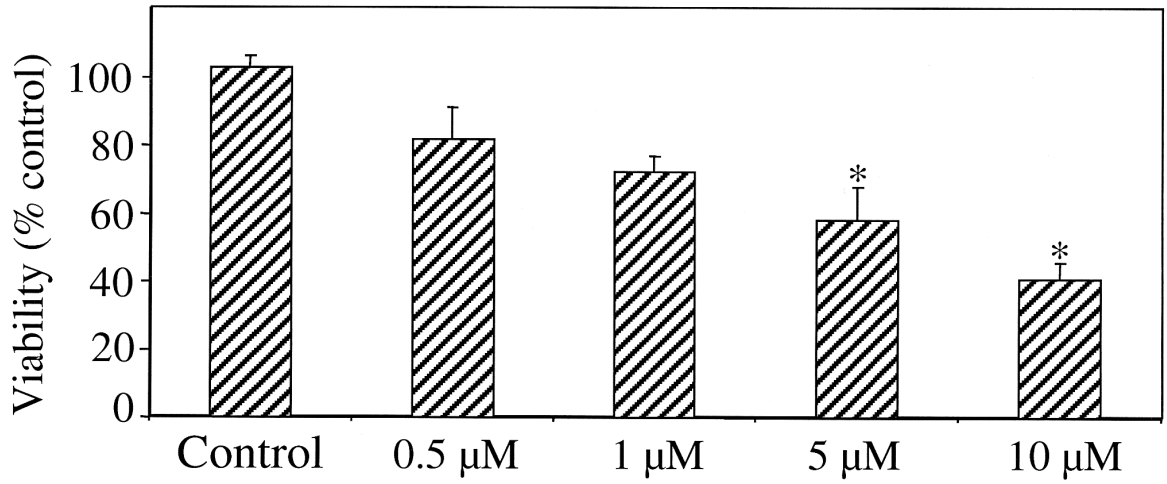

Fig.8

Synthetic miniprion PrP106

Valentina Bonetto, Tania Massignan, Roberto Chiesa, Michela Morbin, Giulia Mazzoleni, Luisa Diomede, Nadia Angeretti, Laura Colombo, Gianluigi Forloni, Fabrizio Tagliavini and Mario Salmona

J. Biol. Chem. published online June 10, 2002
